ISSN 1995-0780, Nanotechnologies in Russia, 2016, Vol. 11, Nos. 9–10, pp. 610–616. © Pleiades Publishing, Ltd., 2016.
Original Russian Text © Andrey S. Orekhov, T.S. Kamilov, Anton S. Orekhov, N.A. Arkharova, E.V. Rakova, V.V. Klechkovskaya, 2016, published in Rossiiskie Nanotekhnologii, 2016, Vol. 11, Nos. 9–10.

Electron Microscopy Characterization of Higher Manganese Silicide Film Structure on Silicon

Andrey S. Orekhov[a, b]*, T. S. Kamilov[c], Anton S. Orekhov[a, b], N. A. Arkharova[a], E. V. Rakova[a], and V. V. Klechkovskaya[a]

[a]*Shubnikov Institute of Crystallography of Federal Scientific Research Centre "Crystallography and Photonics," Russian Academy of Sciences, Leninskii pr. 59, Moscow, 119333 Russia*

[b]*National Research Center "Kurchatov Institute," pl. Akademika Kurchatova 1, Moscow, 123182 Russia*

[c]*Tashkent State Technical University, ul. Universitetskaya 2, Tashkent, 100095 Uzbekistan*

**e-mail: andrey.orekhov@gmail.com*

Received February 1, 2016; accepted for publication February 15, 2016

Abstract—The structure and composition of higher manganese silicide (HMS) films on Si(111) substrate are studied by high-resolution transmission electron microscopy, electron diffraction, and energy-dispersive X-ray spectroscopy. The formation of Mn_4Si_7 HMS film by the deposition of the gas-phase manganese onto silicon at 1040°C is observed. The film/substrate interface is semicoherent and does not contain any intermediate layer. The interface structure is refined by computer simulation. The orientation relationship $(\bar{1}\bar{2}4)[443]Mn_4Si_7 \parallel (1\bar{1}\bar{1})[101]Si$ between the film and substrate is determined.

DOI: 10.1134/S1995078016050128

INTRODUCTION

Currently the issue of energy resource economy is draws much attention. Thereby materials possessing thermoelectric properties attract increased interest. The $MnSi_{1.75}$ HMS is the most promising material due to good thermoelectric characteristics in the 20–800°C temperature range, low price and easiness of manufacturing. The HMS films play an important role in thermobattery and other thermoelements fabrication [1]. Such films already find application in micro- and nanoelectronics, optoelectronics, microsensorics and also are very promising for spintronics [2]. Deep understanding of HMS films formation mechanism is essential for device fabrication and for Mn–Si system solid-phase reactions at elevated temperatures. The Mn–Si binary phase diagram has a region of homogeneity with 5–10 at % width in the range of 64–66 at % Si. Therefore, the HMS phases with various stoichiometry (Mn_4Si_7, $Mn_{11}Si_{19}$, $Mn_{15}Si_{26}$ and $Mn_{27}Si_{47}$) called the Nowotny phases are exists [3–6]. The systematic precipitation of the MnSi manganese monosilicide phase in the form of lamellar layers oriented normally to the $\boldsymbol{c}_{HMS}$ axis is the microstructure feature of the bulk HMS crystals. The MnSi phase, unlike the Mn_4Si_7 HMS, is electrical conductor with high thermal conductivity and low figure of merit [7] and therefore as believe negatively affects to the thermoelectric properties of HMS crystal in general [8].

A large number of studies have been devoted to the HMS films structure and composition analysis but in fact data quite controversial [9–11]. At present only high-resolution electron microscopy techniques could provide the detail information about chemical and phase composition, the HMS grains orientation and the film/substrate interface structure. These data are especially required for the thermoelectric HMS films production technology development with predictable electrophysical properties.

The formation of Mn_4Si_7 HMS film with 15–20 μm grain size is shown as a result of manganese deposition on the silicon single crystal substrate in an evacuated quartz ampoule at 1040°C [12]. The Mn_4Si_7 HMS phase possesses optimal thermoelectric characteristics among all manganese silicides and is suitable for the development of medium-temperature thermoelectric generators [13]. However, initial stages of HMS film growth and atomic structure analysis of the film/substrate interface have not been sufficiently studied yet.

In this work we have studied the structure of microcrystalline HMS films formed in the process of the interaction of silicon single crystal substrate with manganese vapors by scanning and transmission electron microscopy techniques. High-resolution transmission electron microscopy allowed to obtain the local information of the film chemical and phase composition and HMS film/substrate interfaces structure.

MATERIALS AND METHODS

HMS Films Growth Procedure

Thin HMS films were grown by deposition of twice-sublimated Mn (the grain sizes were no larger than 50 μm) in gas phase onto *p*-type Si(111) single crystal substrate (resistivity ρ = 10 Ohm cm) at 1040°C temperature in a sealed quartz ampoule evacuated to 10^{-4} Torr pressure. The Si substrates were preliminarily cleaned from the natural oxide by etching in a solution of HNO_3 : HF = 1 : 4 and rinsed in deionized water. The ampoules were placed into a heated to 1040°C furnace, which was chosen on the basis of the results of [12]. Manganese is a sublimating metal, i.e., it evaporates from a solid state at the abovementioned temperature and its vapor equilibrium pressure amounts to 10^{-2} Torr. The growth process duration was varied from 20 to 40 min, after that ampoules were cooled to the room temperature.

Characterization of HMS Film Structure

The morphology, microstructure, and chemical composition of the samples were studied by scanning electron microscopy (SEM) and energy-dispersive X-ray spectroscopy (EDS) on a Quanta 200 3D microscope (FEI, The Netherlands) at 5–30 kV acceleration voltage in the secondary and backscattered electron modes. Transmission electron microscopy (TEM), electron diffraction (ED), high-resolution transmission electron microscopy (HRTEM) and high-resolution scanning transmission electron microscopy (HRSTEM) were used for chemical and phase composition analysis at a nanoscale. The study was done in TITAN 80-300 TEM/STEM microscope (FEI, The Netherlands) at 300 kV acceleration voltage. The images at STEM mode were recorded by a high-angle annular dark-field (HAADF) detector (Fishione, USA). The use of a probe spherical aberration corrector (CEOS, Germany) allows to obtain the HRSTEM images with a resolution up to 0.08 nm. A chemical analysis was carried out using an energy-dispersive X-ray spectrometer (EDAX, USA) and an ES Vision/TIA software (FEI, The Netherlands).

In order to the HMS films cross sections structure study by SEM the samples were cutted on a Leica TIC by three Ar^+ ion beams at 1–5 kV acceleration voltage through a protective mask. The thin samples for TEM studies were prepared by a focused ion beam (FIB) technique in a dualbeam (FIB/SEM) scanning electron microscope HELIOS NanoLab 600 (FEI, The Netherlands) at 5–30 kV acceleration voltage. In order to remove the disturbed amorphous layer the samples were additionally thinned at 2 kV acceleration voltage.

The structure of the film and substrate at a nanoscale was analyzed using the fast Fourier transformation (FFT) of the local regions of HRTEM images. The measured interplanar distances and the angles between the crystallographic directions were compared with the known data for the manganese silicides phases [3–6]. The electron diffraction patterns and calculated HRTEM images were simulated for the known structural data of manganese silicide using JEMS-Java Electron Microscopy Software [14] in according to the optical parameters of the transmission electron microscope.

RESULTS AND DISCUSSION

Morphology of the Films

SEM images of the sample surface at different stages of HMS film nucleation and growth are shown in Fig. 1. Small islands of manganese silicide with the 20–50 nm size (shown by the arrows in Figs. 1a and 1b) are formed at the 1040°C temperature as a result of manganese and silicon interaction. Such islands merge into larger ones (up to 1 μm in size), rounded shape with a crystalline facets associated with a single crystal structure. Stepped "craters" in the substrate between large islands are observed (Fig. 2). Small non-faceted islands located mainly at the base of the large ones are also observed on the substrate. When the time of manganese deposition increases, the complete fusion of the islands and the formation of a continuous HMS film takes place (Fig. 1c). The electron microscopy images of the HMS film surface obtained at different growth stages indicate that the formation of the islands occurs according to the Volmer–Weber growth mode [15].

The initial stages of HMS film growth as a result of manganese deposition on the silicon single crystal substrate were not considered earlier. The data allow us to propose the following scheme of film formation. Manganese atoms deposited from the vapor–gas phase onto the substrate interact with silicon atoms and form nuclei and small islands of manganese silicide (Fig. 3a). Further, small islands grow due to the migration of the molecules along the substrate and form larger islands (Fig. 3b). Stepped craters arise in certain substrate regions as a result of the diffusive mass transport of silicon and Mn_4Si_7 molecules to the islands that are forming (Figs. 2, 3c). Continuous film formed as a result of island growth and fusion (Fig. 1c). The observed the HMS films initials growth stages and proposed scheme of film formation are in good agreement with the data of [16].

Structure of the Samples

According to the EDS microanalysis, the film composition at all growth stages was homogeneous and corresponded to the $MnSi_{1.7}$. The structure of HMS islands was studied by TEM. Figure 4 shows the

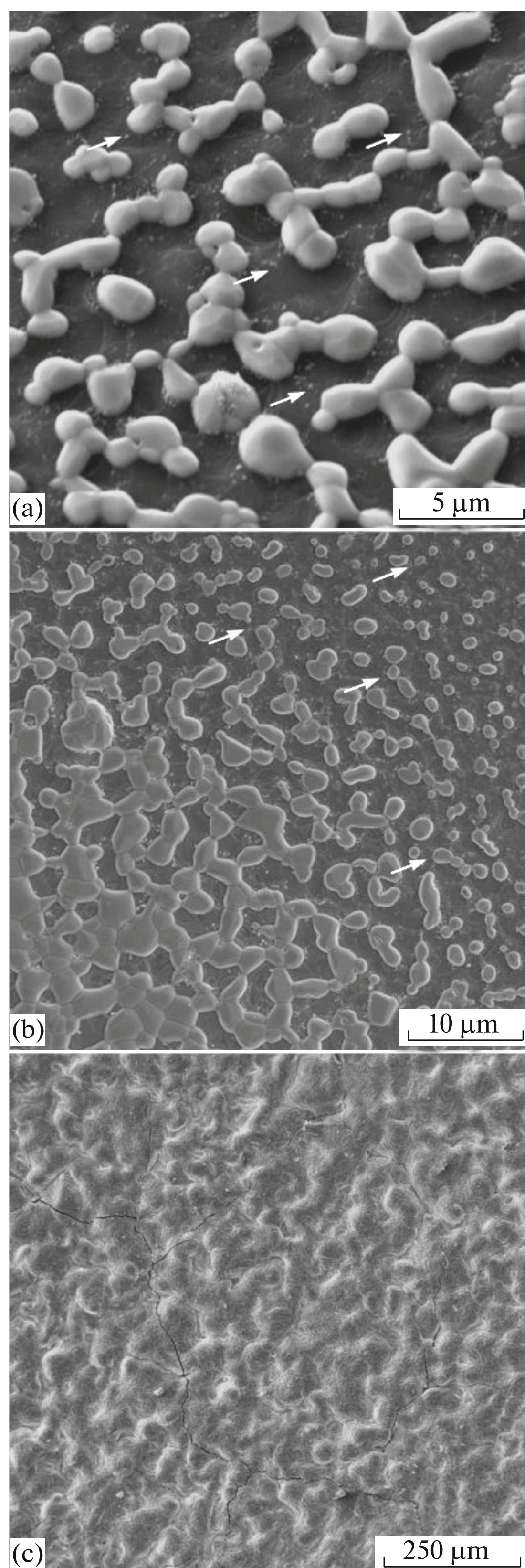

Fig. 1. Electron microscopy images of the surface at different stages of HMS-film formation: formation of nuclei and small islands of manganese silicide (shown by arrows) and their coalescence (a), fusion and aggregation of the islands (b), and solid film (c).

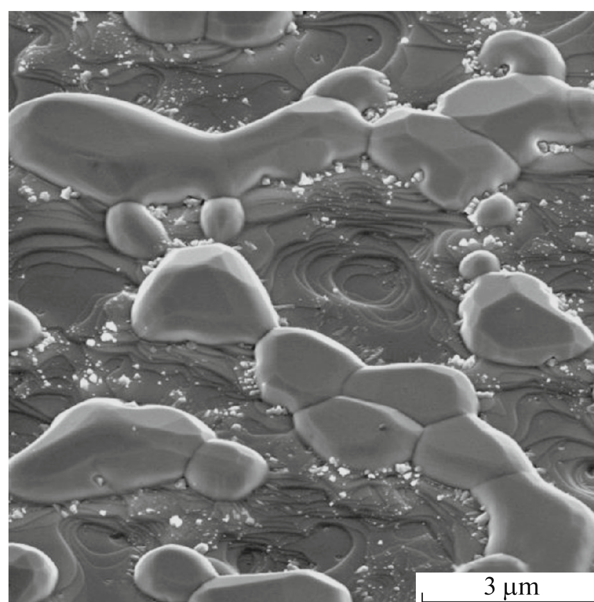

Fig. 2. Magnified image of the sample surface; single faceted islands and their aggregates are seen. Stepped "craters" are formed as a result of the surface diffusion of Si atoms and Mn_4Si_7 molecules.

images of thin cross sections of HMS islands. Round islands up to 1 μm in diameter have an elliptical shape with an aspect ratio of ~0.5. The islands are immersed in the substrate to a depth of ~200 nm. The analysis of a TEM images of the cross sections has shown that the HMS islands possess a single crystal structure. The height of a single islands and small islands aggregates is practically the same and reach to ~500 nm. Such island height is probably preferable for this growth method. The craters depth between the islands formed during film deposition is up to 200 nm.

The phase and chemical analysis of HMS islands thin cross sections confirmed the absence of the inclusions of other phases in particular manganese monosilicide MnSi. The MnSi phase is often observed both in bulk HMS crystals and in sintered polycrystalline samples [8, 17]. Manganese monosilicide was found early as rounded inclusions in HMS islands and in thin films prepared by Mn deposition on silicon substrate in a quartz reactor under continuous evacuation [18]. The absence of MnSi precipitates in the studied films indicates that the chosen growth mode is optimal and can be recommended for practical applications.

The analysis of a series of electron diffraction patterns from the HMS grains and a comparison of interplanar distances and angles between the reciprocal lattice vectors with the data for the known HMS phases have shown that our films possess a tetragonal structure ($P\overline{4}c2$ space group) with the unit cell parameters $a = 0.552$ nm and $c = 1.751$ nm, which is in agreement with the results of [3].

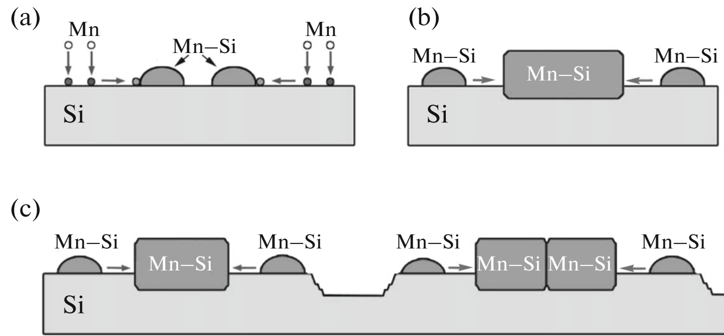

Fig. 3. Schematic representation of the process of manganese silicide film formation on silicon: the first stage is the formation of nuclei and small islands of manganese silicide (a), the second stage is the growth of the islands and their coalescence (b), and the third stage is the fusion of the islands with each other and formation of a solid film (c).

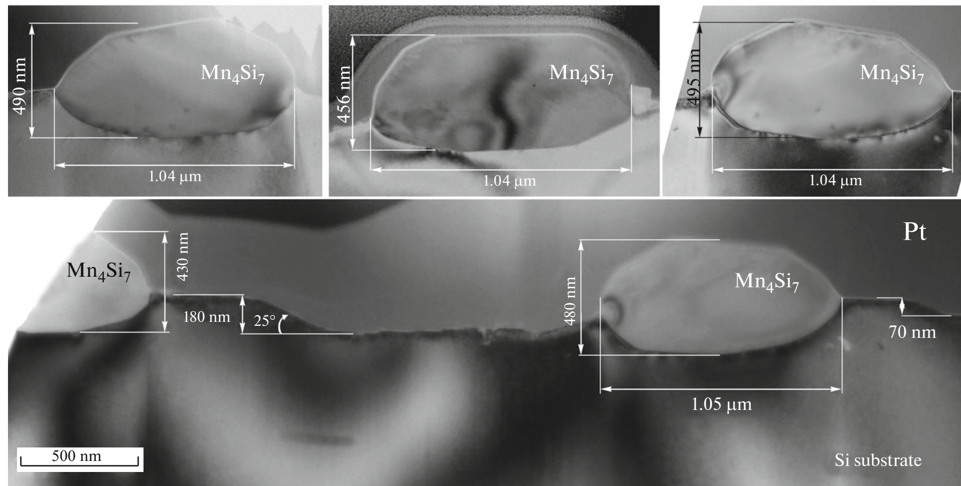

Fig. 4. TEM images of the cross sections of HMS grains on a silicon substrate.

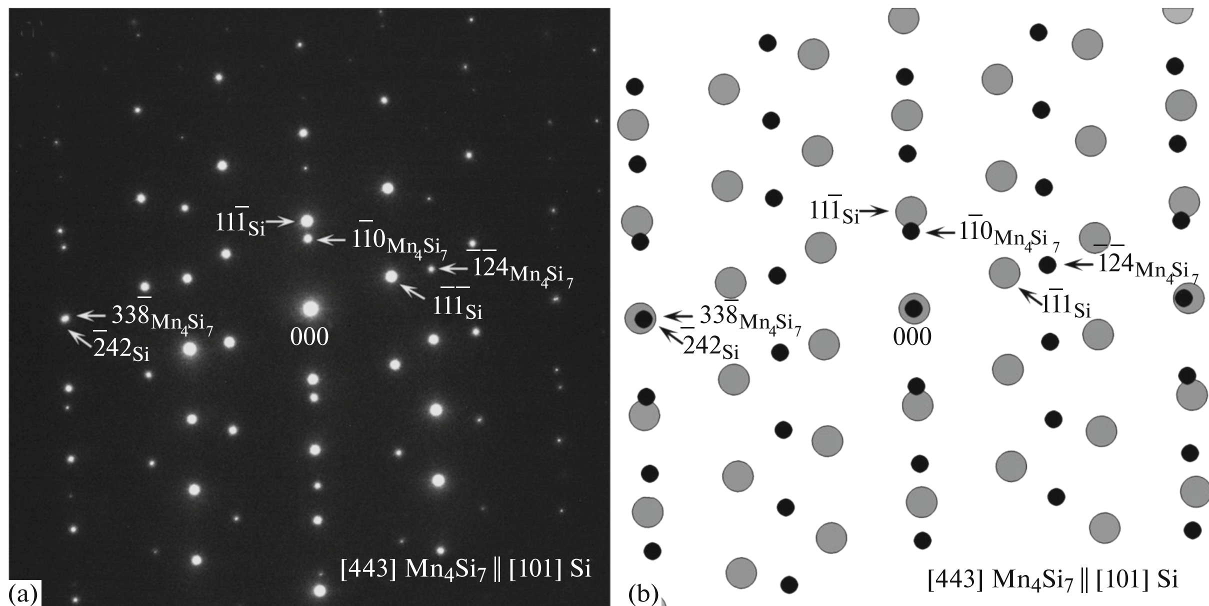

Fig. 5. Electron diffraction pattern from the HMS film/Si substrate (a) and corresponding calculated electron diffraction pattern (b).

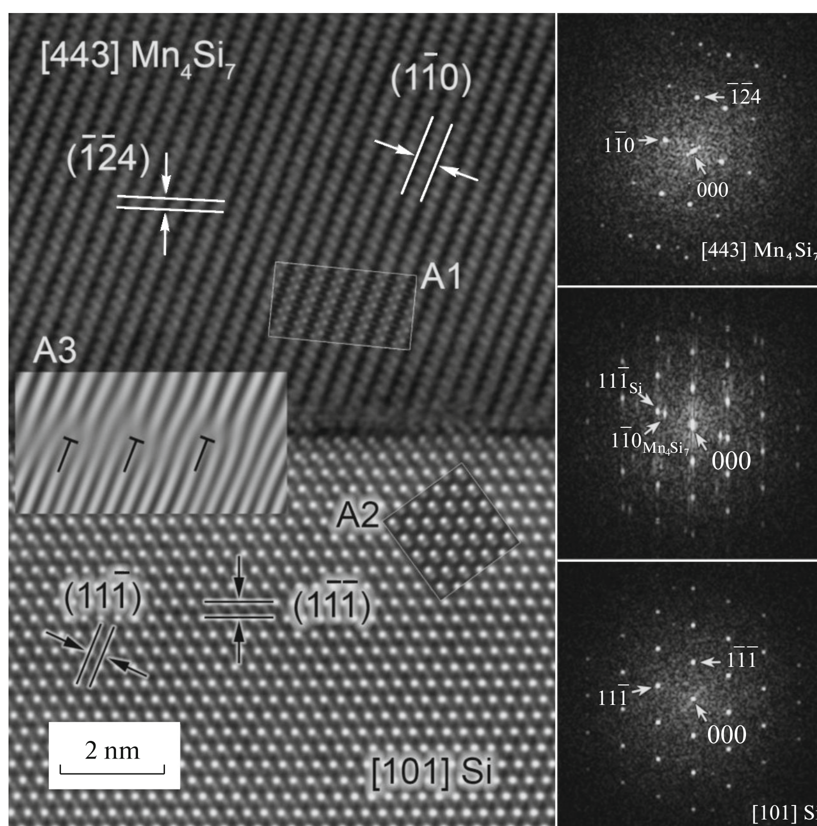

Fig. 6. HRTEM image of the HMS film/Si substrate interface (on the left). Diffractograms obtained by the Fast Fourier Transformation of the selected regions in HRTEM images: HMS film, interface, and silicon substrate (on the right). Inserts A1 and A2 are the simulated HRTEM images when Mn_4Si_7 [443] and Si [101] directions are parallel to the incident electron beam. Insert A3 is the filtered HRTEM image according to the Si(11$\bar{1}$) and Mn_4Si_7(1$\bar{1}$0) reflexes revealing a network of misfit dislocations at the interface.

Film/Substrate Interface

Structure of film/substrate interfaces plays the key role in the processes of thermal and electric transport in films of thermoelectric materials. Phonon scatering, carriers and thermal transport depends on the interface structure type (coherent, semicoherent, or non-coherent). All these processes essentially affect the thermoelectric properties of the crystal. The structure of the HMS film/substrate interfaces was studied by electron diffraction and HRSTEM techniques. Figure 5a shows the electron diffraction pattern from the HMS film/Si substrate interface. An analysis of the electron diffraction data has shown that Si[101] and Mn_4Si_7[443] directions are parallel to the incident beam. The film/substrate interface is parallel to the Si(1$\bar{1}\bar{1}$) plane and forms an angle of ~4° with the Mn_4Si_7($\bar{1}\bar{2}$4) plane. Thus, it is possible to define the following approximate orientation relationship: ($\bar{1}\bar{2}$4)[443]Mn_4Si_7 ∥ (1$\bar{1}\bar{1}$)[101]Si. Its refinement was carried out by superposing stereographic projections of Mn_4Si_7 and Si crystals under parallel directions [443]Mn_4Si_7 ∥ [101]Si and planes ($\bar{1}\bar{2}$4)Mn_4Si_7 ∥ (1$\bar{1}\bar{1}$)Si. Close location of these directions and planes at superposing stereographic projections confirms the right electron diffraction analysis (Fig. 5b).

The HMS and silicon interplanar distances misfit could be estimated in according to electron diffraction data. The Mn_4Si_7(2 2 15) plane is almost perpendicular to the Mn_4Si_7[443] direction, while the Si(101) plane and Si[101] direction are normal. The value of interplanar distances misfit can be derived by equation $\varepsilon = (d_{Mn_4Si_7} - d_{Si})/((d_{Mn_4Si_7} + d_{Si})/2) \times 100\%$. Taking into account that $d(2\ 2\ 15)_{Mn_4Si_7} = 0.101$ nm and $d(101)_{Si} = 0.384$ nm we have $\varepsilon = 5\%$.

The HRTEM image of the interface is shown in Fig. 6. A local geometric analysis of the near-interface regions structure was carried out by the fast Fourier transformation. The interface is semicoherent with a network of misfit dislocations. The indexed diffractograms are shown in the Inserts in Fig. 6. Refinement of the phase, sample orientation with respect to the incident electron beam and crystal thickness estimation

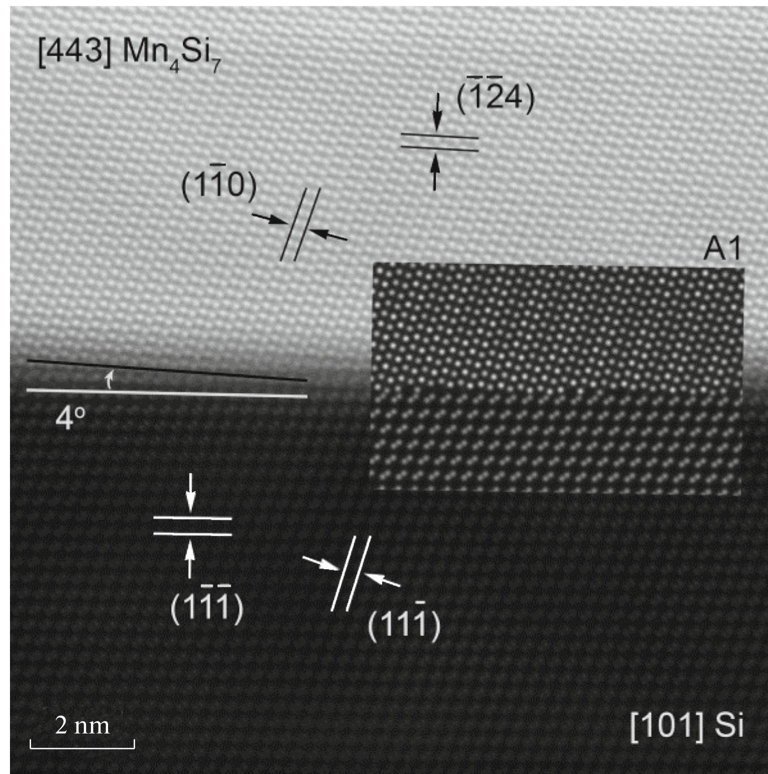

Fig. 7. HRSTEM image of the interface with a contrast proportional to the atomic number of the substance. Insert A1 is the calculated HRSTEM image in accordance with the atomic model of the interface.

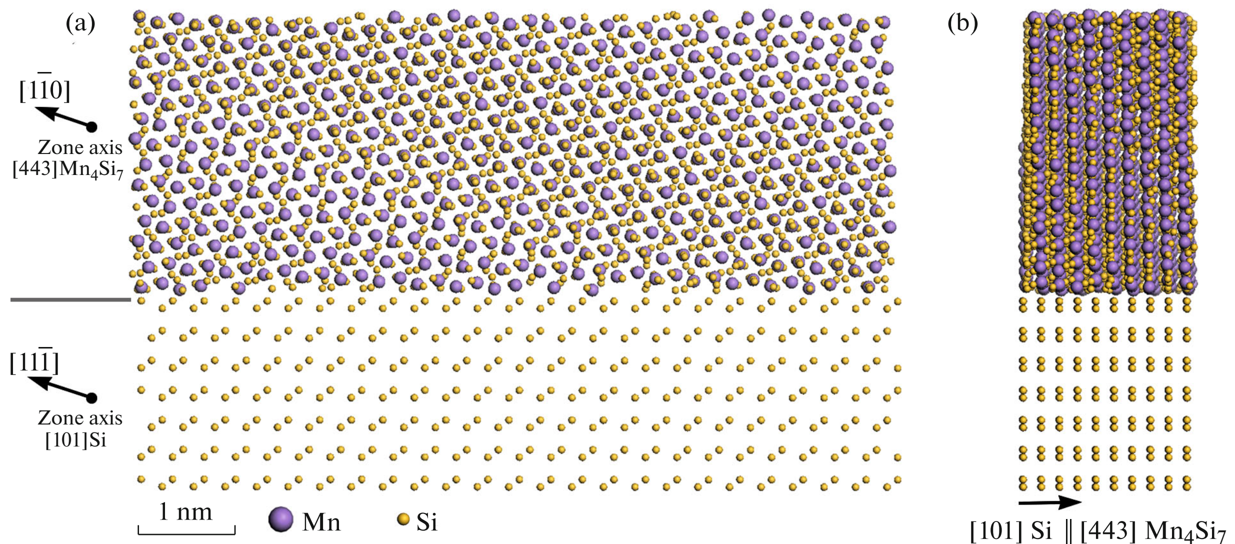

Fig. 8. Atomic model of the HMS/Si substrate interface. The arrows indicate the corresponding directions in Mn_4Si_7 and Si crystals. The projections in (a) and (b) are turned with respect to each other by 90°.

were carried out by HRTEM images simulation. The series of HRTEM images were calculated as a function of the sample thickness and the defocus value for the Mn_4Si_7 phase and Si substrate. A good agreement between the calculated and experimental data was obtained at 18.34 nm crystal thickness and 30 nm

defocus for Mn_4Si_7. For silicon substrate at 21.57 nm crystal thickness and 30 nm defocus value (Inserts A1 and A2 in Fig. 6). On a filtered at $Si(11\bar{1})$ and $Mn_4Si_7(1\bar{1}0)$ reflexes HRTEM image a network of misfit dislocations formed due to different interplanar distances at the interface is revealed (Insert A3 in Fig. 6).

By applying HRSTEM technique we have obtained an image of atomic columns with a contrast proportional to the atomic number of the element (so-called Z-contrast). The region of HMS film and substrate contact is shown in Fig. 7. The silicon atomic number Z_{Si} is 16 and for manganese Z_{Mn} is 25. Thus a light contrast in the upper part of the image corresponds to the manganese atomic columns. The film/substrate interface is parallel to the $Si(11\bar{1})$ plane and is at an angle of ~4° to the $Mn_4Si_7(\bar{1}\bar{2}4)$ plane. A sharp different of image contrast at interface is indicates the intermediate layer absence.

A three-dimensional atomic model of the interface structure was built in correspondence of the defined orientation relationships and HRSTEM images (Fig. 8). The HRSTEM image simulation was calculated for proposed model of the interface (Insert A1 in Fig. 7). A good agreement between the calculated and experimental images proves the correctness of the proposed model of the interface.

CONCLUSIONS

In this paper the morphology and structure of HMS films on silicon is analyzed. As a result of manganese deposition onto silicon substrate at 1040°C the HMS films with Mn_4Si_7 tetragonal structure ($P\bar{4}c2$ space group, a = 0.552 nm, and c = 1.751 nm) are formed. An analysis of different stages of film formation allowed us to propose a scheme of HMS film formation on silicon. By electron diffraction, HRTEM, and HRSTEM the structure of the film/substrate interface is studied. It was shown that the interface is semicoherent with a network of misfit dislocations. The absence of intermediate layer at HMS film/Si substrate interface is shown by HRSTEM technique. On the basis of the experimental data a three-dimensional atomic model of the interface structure is proposed. Simulated high resolution transmission electron microscopy images are in good agreement with the experimental data, that prove the correctness of the proposed interface model.

ACKNOWLEDGMENTS

This work was carried out with partial financial support (scholarship from the President of the Russian Federation for young scientists and postgraduate students no. SP-1404.2016.1) using equipment of the Center for Collective Use of the Institute of Crystallography of the Russian Academy of Sciences and Resource Center of probe and electron microscopy of Kurchatov complex of NBIC technologies.

REFERENCES

1. T. S. Kamilov, V. V. Klechkovskaya, B. Z. Sharipov, I. V. Ernst, and V. K. Zaitsev, *Electrical and Photoelectrical Properties of Heterophase Structures Based on Silicon and Manganese Silicide* (MERIYUS, Tashkent, 2014) [in Russian].
2. C. A. Nolph, E. Vescovo, and P. Reinke, Appl. Surf. Sci. **255**, 7642 (2009).
3. U. Gottlieb, A. Sulpice, B. Lambert-Andron, and O. Laborde, J. Alloys Comp. **361**, 13 (2003). ICSD #97393
4. O. Schwomma, A. Presinger, H. Nowotny, and A. Wittmann, Monatsh. Chem. **95**, 1527 (1964). ICSD #43280
5. H. W. Knott, M. H. Muller, and L. Heaton, Acta Crystallogr. **23**, 549 (1967). ICSD #15339
6. G. Zwilling and H. Nowotny, Monatsh. Chem. **104**, 668 (1973). ICSD #23789
7. L. I. Petrova, M. I. Fedorov, V. K. Zaitsev, and A. E. Engalychev, Inorg. Mater. **49**, 355 (2013).
8. L. M. Levinson, J. Solid State Chem. **6**, 126 (1973).
9. S. Teichert, S. Schwendler, D. K. Sarkar, A. Mogilatenko, M. Falke, G. Beddies, and H. J. Hinneberg, J. Cryst. Growth **227**, 882 (2001).
10. A. Mogilatenko, M. Falke, S. Teichert, S. Schwendler, D. K. Sarkar, and H. Hinneberg, Microelectron. Eng. **60**, 247 (2002).--
11. M. Kohira, Y. Souno, T. Matsuyama, H. Tatsuoka, I. J. Ohsugi, I. A. Nishida, and H. Kuwabara, Appl. Surf. Sci. **216**, 614 (2003).
12. V. V. Klechkovskaya, T. S. Kamilov, S. I. Adasheva, S. S. Khudaiberdyev, and V. I. Muratova, Crystallogr. Rep. **39**, 815 (1994).
13. T. S. Kamilov, D. K. Kabilov, I. S. Samiev, Kh. Kh. Khusnutdinova, R. A. Muminov, and V. V. Klechkovskaya, Tech. Phys. **50**, 1102 (2005).
14. P. Stadelmann, The Java Electron Microscopy Software JEMS (2012). http://cimewww.epfl.ch.
15. M. Volmer and A. Weber, Z. Phys. Chem. **119**, 277 (1926).
16. S. N. Kukushkin and A. V. Osipov, Phys. Usp. **41**, 983 (1998).
17. Z. Wang, Y. Wu, and Y. He, Int. J. Mod. Phys. B **18** (1), 87 (2004).
18. E. I. Suvorova and V. V. Klechkovskaya, Crystallogr. Rep. **58**, 854 (2013).

Translated by R. Litvinov